



SPE/ISRM 47401

Viscous Rheology and State of Stress in Unconsolidated Sands

C.T. Chang and M.D. Zoback, SPE, Stanford University

Copyright 1998, Society of Petroleum Engineers, Inc.

This paper was prepared for presentation at SPE/ISRM Eurock '98 held in Trondheim, Norway, 8-10 July 1998.

This paper was selected for presentation by an SPE Program Committee following review of information contained in an abstract submitted by the author(s). Contents of the paper, as presented, have not been reviewed by the Society of Petroleum Engineers and are subject to correction by the author(s). The material, as presented, does not necessarily reflect any position of the Society of Petroleum Engineers, its officers, or members. Papers presented at SPE meetings are subject to publication review by Editorial Committees of the Society of Petroleum Engineers. Electronic reproduction, distribution, or storage of any part of this paper for commercial purposes without the written consent of the Society of Petroleum Engineers is prohibited. Permission to reproduce in print is restricted to an abstract of not more than 300 words; illustrations may not be copied. The abstract must contain conspicuous acknowledgment of where and by whom the paper was presented. Write Librarian, SPE, P.O. Box 833836, Richardson, TX 75083-3836, U.S.A., fax 01-972-952-9435.

Abstract

Observations of triaxial creep and stress relaxation of unconsolidated reservoir sands imply markedly different static and dynamic moduli and may explain observations of very low differential stresses found in the Wilmington Field, CA, the Gulf of Mexico, and elsewhere. Triaxial testing performed on 1 inch plugs of reservoir sands under both stress- and strain-controlled conditions show transient stresses and strains. All tests were performed under dry or drained conditions to eliminate poroelastic effects. We previously observed creep under hydrostatic stress conditions in these unconsolidated sands. The resulting strain vs. time curves could be fit with a standard linear solid viscoelastic model that had a relaxation time of about 10 hours. The data demonstrates the rock's ability to dissipate stress through relaxation and creep. The reservoir material shows viscoelastic rheological behavior in both creep and relaxation tests which appears to be related to the presence of intergranular clay. Measurements of the static Poisson's ratio under large strains yielded values ~ .29 which suggests that the particles in the matrix efficiently coupled the principle strains.

Introduction

Time dependent deformation of unconsolidated sediments is traditionally understood to arise from pore fluid expulsion in saturated earth materials^{1,2}. Although many accounts have been published relating the viscous behavior of soils at shallow depth associated with dewatering, there have been few studies of time-dependent deformation of poorly consolidated

rocks under drained or dry conditions at the low stresses encountered in hydrocarbon reservoirs. Viscous deformation of unconsolidated sands can creep during compaction at elevated pressures³ and related this behavior to time dependent moduli. They do not necessarily require differential stresses, saturation, or high temperatures. This study examines time varying stress relaxation in unconsolidated sediments under drained conditions and demonstrates how they can be related to differential stress in unconsolidated reservoirs.

Highly variable and often very low differential stresses are commonly seen in poorly consolidated sands (e.g. Finkbeiner and Zoback⁴). This results in estimates of principle stress magnitudes that are often explained if poorly consolidated sands were modeled with viscoelastic rheology.

There are numerous studies of strength and deformation of unconsolidated or weakly consolidated rocks in the rock mechanics literature. These tests are typically at pressures more relevant to those encountered in hydrocarbon recovery^{5,6,7,8}. However, very few accounts report the existence of time dependent deformation when dealing with the compressive behavior of sediments. Although time dependent deformation is observed in investigations (such as Kang⁸), the data show flat plateaus on stress versus strain curves that are not addressed directly. As in the soil mechanics literature, if dependent deformation is addressed, it is associated with fluid expulsion during consolidation. Such tests are typically using partially drained conditions arising from low permeability such as Lo and Lee⁹ who observed time dependent deformation in saturated shales. Poroelastic phenomena associated with low permeability rocks are not relevant when studying highly permeable rocks.

Two investigations that examined time dependent deformation in poorly consolidated rock under drained conditions are Dudley et al¹⁰, and Finkbeiner and Zoback⁴. These investigations report time dependent deformation of unconsolidated reservoir rocks at pressures and strains under triaxial loading configurations. Their samples were partially drained and highly permeable. The high permeability prevented the development of unrelaxed pore pressure during consolidation. These triaxial loading tests ex-

creep strain that could be fit with a power law creep model. Their study observed the creeping behavior of sand at low temperatures. These observations of time dependent creep in Gulf of Mexico turbidites and river sands suggested that the rocks have a viscoelastic character. However, their boundary conditions were constant axial or hydrostatic load and zero pore pressure, which prevented the observation of stress relaxation or transient pore pressure, thus leaving the question of time dependent stress unanswered.

Poisson's ratio should give some indication of an unconsolidated sand's degree of fluidity. Poisson's ratio describes how well the principle strains in a material are coupled. Spencer¹² provided extensive experimental results showing that clean dry sands tested in the laboratory using ultrasonic techniques had Poisson's ratios between .15 and .20. These are much lower than one would expect from a matrix that "flows" as an incompressible fluid which has a theoretical value of 0.50. Karig⁸ performed static experiments on sediments from the Nankai trench that gave values of approximately .20 to .25. To observe coupling between the principle strains requires deforming the material past its virgin consolidation state. This is not captured by ultrasonic measurement techniques that use smaller strain perturbations. Large strain perturbations would be a simple way to observe the degree of coupling between ϵ_{11} and ϵ_{22} thus determining the degree of fluidity. The static Poisson's ratio is as important as the ultrasonic information because it governs how unconsolidated reservoir rock behaves under large displacements and over long time periods.

Viscoelastic theory states that if a material creeps, then it should relax given the proper boundary conditions^{13,14}. Creep is time dependent deformation under constant stress while relaxation is stress decay under constant strain. Viscoelastic theory states that if a material creeps viscoelastically, the relaxation stress can be derived mathematically (See Appendix). This means that if our sample is viscoelastic, then we should observe time varying stresses under constant strain boundary conditions. To illustrate the relationship between creep and relaxation, consider the creep strain in Fig. 1. By fitting the data with a standard linear solid model (Fig. 1 inset), we can get a creep function for the material. Using viscoelastic theory (e.g. Tchoegel¹⁵ and Appendix) we can use the creep data to calculate the expected time dependent stress as seen in Fig. 2.

In the following study, we present our observations of time dependent deformation under triaxial loads. This presents compelling evidence of viscoelasticity. Viscoelastic creep (but not stress relaxation) under hydrostatic pressures in unconsolidated sands has already been documented in Chang et al². To demonstrate the phenomena under triaxial loads, we extended our study to tests with both constant stress and constant strain boundary conditions. Data from a variety of different triaxial tests demonstrate the different phenomena arising from a viscous rheology. The resulting data presents

clear evidence for rock viscoelasticity under

Experimental Procedure

The samples used in this study were all unconsolidated described in the Table 1. All samples were quartz sands with mean grain of 300 μ m. Porosities were between 30 and 40%. The samples containing less than 10% clay.

The core samples of unconsolidated sand were obtained from two hydrocarbon reservoirs. The samples were obtained from the Wilmington Beach, California from a depth of approximately 10000 feet in wells UP941B and 169W. The Lentic samples were obtained from the South Eugene Island field in the Gulf of Mexico from a depth of 7883 feet in well SEI-613/A12. Ottawa sand samples were prepared in the laboratory. The cores from the laboratory were jacketed in PVC at the wellsite and tested to preserve the natural state of the rock. The Lentic samples came from a refrigerated storage.

The samples were extracted from the core by coring at room temperature with steel tubing. The sand was extruded into soft polyolefin jacketed tubes. The specimen was 1 inch in diameter and 2 inch long. The samples to be tested "dry", residual heavy oil was removed from the samples by flushing first with methanol and then with air to dry the porespace. The sample was then wired to a transducer stack and placed in a pressure vessel for testing under room-dry conditions and room temperature.

The Ottawa sand Montmorillonite clay was prepared by mixing Ottawa sand with 5% clay by volume. The laboratory grade clay was first wetted then allowed to dry with air circulation for 24 hours before testing. The absence of viscous effects with the Ottawa sand clay motivated this procedure. The residual water content below 5% by gravimetric analysis estimated by oven drying. The jacketing enclosed the mixtures while the sand was under the loading endcaps.

The loading system was a triaxial cell instrumented with axial strain and radial strain gauges. A PC based data acquisition system controlled the test. Stress, strain, temperature, and pore pressure were measured. An internal load cell measured the differential load. The temperature was maintained at room conditions. Hydraulic controllers allowed for precise stress ramps. Feedback circuitry connected to the load cell and pore pressure measurement system allowed experiments to be run under constant stress boundary conditions as well.

(I) Creep Testing.

Constant load creep tests were performed by increasing the axial load at 10 MPa/minute and then holding the load constant while maintaining a constant confining pressure.

Maintaining a constant axial load resulted in axial creep. PC data acquisition monitored the transient creep response for up to 10 hours.

Uniaxial creep strain experiments were performed similarly but rather than maintaining a constant confining pressure, the radial strain gauge adjusted the confining pressure to maintain constant radial strain while holding the differential load constant.

(II) Relaxation Testing.

The analog of creep can be achieved by holding the axial strain boundary condition constant following a step displacement of the axial piston. Relaxation tests were performed under triaxial conditions by step loading the stress and allowing the axial piston to advance to a predetermined position. A closed loop feedback controller maintained that position by adjusting the axial stress. An internal load cell directly measured the vertical load on the sample. PC data acquisition performed prior to and following loading recorded both the impulse and transient response of the displacement and load. These tests are run dry and drained. The Ottawa sand/5% Montmorillonite clay sample was run "room dry" with pre-wetted laboratory grade Montmorillonite (see description in Chang et al²).

(III) Pore Pressure Transient Tests.

The pore pressure transient testing was performed in a manner similar to (II). The major difference was that the samples were saturated. The pore pressure control system was shut in to maintain constant pore volume. These were essentially undrained triaxial and uniaxial tests. The differential load was stepped and held at a nominal value and the axial displacement was allowed to creep at constant confining pressure in the triaxial case, or constant radial strain in the uniaxial case. The PC acquisition system monitored the time history of the pore pressure prior to and following the stress perturbation. These tests were run saturated with denatured alcohol to avoid chemical interactions with the rock fabric.

(IV) Poisson's Ratio by stress and strain.

To determine Poisson's ratio at large displacements, a direct measurement of principle strains (axial and radial) is required during triaxial loading. By measuring the stress ratio under uniaxial strain, we can also estimate the Poisson's ratio assuming linear elasticity of the sample. Under uniaxial strain loading, the sample was monitored while increasing the confining pressure to determine the stress ratio up to 27 MPa of vertical stress. Both measurements are large strain observations of the degree of coupling between the principle strains under large displacements.

Results of Laboratory Testing

As in the hydrostatic loading cases, the rock creep deformation in uniaxial and triaxial configurations while pausing loading ramps constant pressures. All of the samples creeped under constant loads in both triaxial stress and uniaxial configurations.

The creep response under triaxial loading resembles that measured under hydrostatic conditions². Table 1 summarizes the relaxation and loading conditions. For the triaxial case, the Lentic sand time constants are shorter than those of the Wilmington.

When testing the Wilmington sample under uniaxial conditions (Fig. 4), the radial strain gauge and pressure controller had a tendency to give a step like response when the sample crept. Since all strain changes were due to perturbations in the sample, controlling the strain measurement (as in the uniaxial strain case) led to the minor instability observed in Fig. 4. Although the data contains more irregularity than the other relaxation tests, in compression, it is evident that the sample creeps under boundary conditions as well.

In the Lentic sand tests, the triaxial and uniaxial creep functions are strikingly similar to triaxial stress, uniaxial strain, and hydrostatic stress tests in the Wilmington sand. The triaxial compression experiment (Fig. 5) fits the creep function of a standard linear solid and is indistinguishable from the measured triaxially and hydrostatically³ on Wilmington sand.

The uniaxial compression of the Lentic sand has a much lower time constant than the other relaxation tests. It equilibrates much faster. Evidently the time constant is simply a function of the boundary conditions. In the Wilmington uniaxial strain test, the difficulty was in controlling the confining pressure using a strain feedback loop. The data. However, the signal is sufficient to demonstrate the effects of creep under uniaxial compression.

Although there isn't a clear connection between the boundary condition and relaxation time, it appears that the Lentic sand sample deforms with a longer time constant than the more stable triaxial cases. All tests have time constants under 13 hours as in the hydrostatic cases. The difference between the uniaxial creep time constants and the triaxial time constants may reflect the instability of the uniaxial tests. Still, the Lentic sand appears to be a soil that equilibrates quickly under triaxial loading.

Triaxial stress relaxation experiments

Under constant strain steps, stress relaxation was measured on both the Wilmington sand samples and the Ottawa sand/Montmorillonite samples. In the Ottawa sand, the transient stress peaked at 36 MPa differential

to equilibrium (Fig. 7) after 5 hours following the step displacement of the axial piston.

The stress, monitored using an internal load cell mounted directly to the sample, decayed exponentially as a function of time and resembled the theoretical predictions made for viscoelastic media (Fig. 2). The sample was under dry and drained conditions. Although the sample displayed some degree of fluidity under compression, the shear stress did not decay to 0 MPa suggesting that the sample does not reach the isotropic stress state. The residual stress after equilibration suggests that there is a static modulus of this material that maintains a finite differential load over time. This indicates that the rock material isn't totally fluid-like.

A similar response is seen in the Wilmington turbidite sample as well (Fig. 8). In this case, the sample stress increased to a transient peak following the step strain axial displacement and then decayed away over a period of several hours. In this case, the hydrostatic stress was held at a constant pressure of 20 MPa. This sample required more strain to obtain the peak stress observed in the Wilmington sample. The Ottawa sand/Montmorillonite sample lost 58% of its initial strain by the time it reached equilibrium. The sample cannot maintain the initial 36 MPa of differential stress indefinitely, however did maintain a finite load over time.

Pore fluid compression experiments

The objective of the pore fluid compression experiments was to observe the transient increase of pore pressure associated with creep compaction under polyaxial stresses. Under polyaxial compression, sealing the pore fluid system maintained constant pore volume minus the effects of fluid compressibility. Following step axial loads in both triaxial stress and uniaxial strain boundary conditions, the acquisition system collected data of axial creep, volumetric strain, and pore pressure.

The triaxial case showed a time dependent increase in pore pressure. This increase was accompanied by pore volume compaction (Fig. 9a) under constant loads as shown in below in Fig. 9b. The flat stress data demonstrates the system's ability to hold the principle stresses constant during the creep process. Pore pressure increased transiently and approached the confining pressure which is also the least principle stress. The experiment was terminated to prevent the sample jacket from rupturing in a "self hydrofracturing" mechanism. The experiment demonstrated the possibility of transient pore pressure changes following deformation events that can change the effective stress state.

The second time dependent pore pressure experiment involved compacting the Lentic sand under uniaxial strain. From the strain history in Fig. 10(a), the majority of the strain occurs during the step increase in differential stress. The axial creep strain follows the instantaneous step in stress for several hours. In this case there was no radial strain given the uniaxial

strain boundary condition.

The stress history is shown in Fig. 10(b). The sample crept axially after a step load of 22 MPa in the vertical direction, the confining pressure balanced the resulting change in horizontal stress due to Poisson's effect. This resulted in a transient increase in hydrostatic stress followed by a transient increase in pore pressure. The pore pressure increase has been attributed to the volume of fluid in the pore pressure plume.

In these experiments the time dependent pore pressure can be connected to the viscous creep of an uniaxial sample under constant load. In both cases, after the sample is perturbed, a transient pore pressure response is observed under undrained conditions. In both experiments, the changes in pore pressure following an instantaneous perturbation lead to transient changes in the stress field.

Estimates of the Poisson's ratio

Poisson's ratio can be measured using the definition of strain ratio. By definition, the Poisson's ratio is the ratio of lateral principle strains under uniaxial stress. A series of measurements of Poisson's ratio was determined for the stress ratio under the assumption that the material is a linear elastic material.

Compressing the Lentic sample under uniaxial strain with constant confining pressure gave a direct measurement of the principle strains. The results of radial and axial strains on the cylindrical plug sample are shown in Fig. 10. The slope of the curve gives the Poisson's ratio which is approximately 0.293. Aside from this being a linear elastic experiment with plastic deformation, this is a direct measurement of the Poisson's ratio. The curvature of the curve in Fig. 11 suggests that the material displays non-linear behavior. Although the curvature suggests a non-linear Poisson's ratio, a linear fit was used on the data to attempt to capture the average value over the range of strains. The localized non-linearity of the curve gives higher and lower estimates of the Poisson's ratio. The linear fit attempts to capture the average value. The higher and lower estimates of 0.293 and 0.20 are superimposed on the plot to indicate the variability in the data associated with this measurement.

Fig. 12 is the strain history of the Lentic sample under uniaxial strain conditions. The strain rate is constant at approximately 1.55e-7/s. This is also the strain rate and approximately equal to the pore pressure strain rate of the sample. The data shows some irregularity at the end of the experiment because the hydraulic confining pressure had trouble coming to equilibrium when the sample was poorly packed. As the material packed more, the pore pressure deformation became more regular (Time > 2.5 hours).

The relationship between vertical and horizontal strains is summarized in Fig. 13. The change in vertical strain is

the horizontal stress increase to maintain uniaxial strain. Assuming the material behaves as a linear elastic solid at times between 2.5 hours and 5 hours where the constitutive behavior is close to linear, we can relate the stress ratio and the Poisson's ratio by

$$\nu = \frac{\Delta P_c}{\Delta P_c + \Delta \sigma_1} \quad (1)$$

Plotting the principle stresses (Fig. 13) and solving for the Poisson's ratio gives a value of approximately 0.272. There is localized nonlinearity on the curve suggesting that the Poisson's ratio isn't constant over the interval. Although the variation between small intervals is evident, a straight line captures the average behavior of the stress ratio well.

In summary, four different types of tests have demonstrated the physical manifestations associated with viscoelastic rheology. Creep tests at constant load exhibited time dependent deformation. Stress relaxation tests on dry samples showed exponentially decaying transient stresses and the tendency for unconsolidated materials to approach isotropic (low shear) stress states over time. Undrained compaction tests under triaxial loads developed transient pore pressure demonstrating the time dependence of effective stress in unconsolidated sediments. High Poisson's ratios are found when compressing the Lentic sand suggesting a flowing rheology.

Discussion

In all of the experiments presented here, unconsolidated reservoir sand and synthetic sand have a viscoelastic character. As predicted from viscoelastic theory and the hydrostatic creep data sets published previously⁷, the creep can diminish differential stresses under constant strain boundary conditions, and pore pressure can increase due to time dependent pore volume compaction. Given this time dependent dynamic rheology, it appears that the rock matrix, with or without pore fluid, will deform viscously under the applied static loads. The Poisson's ratio measured under large scale strains indicates that this may be occurring by granular flow.

The triaxial stress relaxation tests confirm that rock stresses can relax over time in the constant strain cases given the proper boundary conditions and rock materials. In Figs. 7 and 8, samples that begin with an instantaneous differential stress of around 30 MPa lose their ability to maintain shear stress over time. The steady state stresses in these cases do not approach zero (isotropic stress) because the rock is viscoelastic, not a viscous fluid. The stress decays to the steady state differential strength of the material which can be related to the static Young's modulus. Because the load bearing capacity of the media decays, it can be thought of as the time dependent strength. Although the sample is not in

failure during these experiments, the relaxation of stress can be regarded as weakening. Over time, the sample loses its ability to carry load by approaching the Ottawa and Wilmington sands.

The Poisson's ratio was higher than that of an elastic crystalline rock material (~ 0.25) but less than an ideal incompressible fluid (~ 0.5), and it is consistent with ultrasonic measurements. Ultrasonic testing provides higher values for the Poisson's ratio which are typical for unconsolidated reservoir rock¹². However, the amplitude ultrasonic wave doesn't move the grains the way as a static test. Because the large strain occurs in space, it increases the interaction between grains. These increases intensify the degradation between the principle strains, hence increasing the Poisson's ratio. Since the materials deform at large strains, it may not be appropriate to compare values to small strain ultrasonic measurements.

Our tests on Ottawa sand samples have shown time dependent deformation comes from some clay added to the matrix². Although the sand is saturated, it is possible that minute amounts of intergranular clay allowed the grains to repack and appeared to be a micro-poroelastic effect. The poroelasticity at the grain boundaries determined constant. Since this process is highly dependent on amounts of residual moisture in the clay, this explains the variation in relaxation time constants found in creep experiments. To test this idea, we compressed a thin piece of the same clay that contained the amount found in the 5% Ottawa sand sample mixture and observed creep displacements of similar magnitude as those observed in the Ottawa sand samples (Fig. 14). This observation clearly demonstrates the relationship between the semi-dry clay and the relaxation time constant.

Even with very low water content, the clay exhibits viscoelastic behavior at high stresses. Our tests on premoistened then dried clay to generate creep curves in the experiments, the porosity often changed because the clay's pore volume gets smaller, the micro-pore residual pore water will consume more of the pore spaces in the clay clusters. This will result in an increase in saturation. Since permeability is low at this scale, it is possible that these micro-pore water are unrelaxed — regardless of the overall sand sample. This type of mechanism as "domain compaction" in the clay mechanics provides an explanation for creep in partially saturated soils. This is true in our samples, the degree of micro-porosity and hence micro-permeability controls the relaxation time constant.

The viscoelastic mechanism controlled the creep rate and strength of our rock samples over time. On the time scale, the rock stress will vary. B

occurs after a sudden perturbation of the stress field, it is most relevant to engineering practices where loading rates and observation periods may last from hours to days. Without understanding this phenomena, it is difficult to make consistent strength estimates using log or seismic measurements alone. A combined analysis including a variety of data types at different frequencies better constrains the time dependent material properties. The stress relaxation experiments suggest that a high frequency measurement will never see the low frequency (long term) modulus or the residual stress. This results in a gross over prediction the sand's stiffness and load bearing capacity.

Conclusions

Deformation experiments performed on the Lentic sand, Wilmington sand, and Ottawa sand/Montmorillonite synthetic samples indicate viscoelastic behavior that is unrelated to pore fluid expulsion or dewatering. This type of mechanism may explain differential stresses of poorly consolidated sand. This mechanism may also explain the differences observed between static and dynamic moduli. The experiments successfully demonstrate viscoelastic behavior in unconsolidated sediments under various types of triaxial loads, and were able to identify that the viscoelastic nature of the sands is related to the presence of intergranular clays.

Nomenclature

- P_c = confining pressure
 ν = Poisson's ratio
 σ_a = axial stress
 σ_d = differential stress
 τ = relaxation time
 ϵ_{11} = axial strain
 ϵ_{22} = radial strain

References

- Bishop, A.W., "The Strength of Soils as Engineering Materials," *Geotechnique* (1966) **16**, pp.91-128.
- Terzaghi, K., "The stability of slopes of natural clay," *Proc. 1st Int. Conf. Soil Mech. Found.Engng., Cambridge, Mass.* (1936) **1**, 161-165.
- Chang, C., Moos, D., Zoback, M.D., "Anelasticity and dispersion in unconsolidated reservoir rocks," *Int. J. Rock Mech. & Min. Sci.*, (1997) **34**, No. 3-4, Paper No.048.
- Finkbeiner, T. and Zoback, M.D., "In situ stress, pore pressure, and hydrocarbon migration in the South Eugene Island field, Gulf of Mexico," paper SPE 47212 presented at the 1998 SPE European Rock Mechanics Meeting, Trondheim, Norway, July 8-10.
- Clough, G.W., Sitar, N., Bachus, R.C., Rad, N.S., "Cemented sands under static loading," *Proceedings of the American*

Society of Civil Engineers (1981) **107**, No. 6.

- Vernik, L., Bruno, M., Boyberg, C., "Empirical relationships for compressive strength and porosity of siliceous rocks," *Rock Mech. Min. Sci. & Geomech. Abstr.* (1981) **680**.
- Yamamoto, J.A., Bopp, P.A., Lade, P.V., "The effect of pore fluid compression of sands at high pressure," *Geotechnical Engineering* (1996), **122**, No. 1.
- Karig, D.E., "Uniaxial reconsolidation tests of mudstones from site 897," *Ocean Drilling Program Results*, (1996) **149**, 363-373.
- Lo, K.Y., Lee, Y.N., "Time-dependent deformation of Queenstown shale," *Can. Geotech. J.*, **27**, 463-474.
- Dudley, J.W., Myers, M.T., Shew, R.L., "Measuring compaction and consolidation of unconsolidated reservoir materials via triaxial testing," *Proc. of Eurock '94 Balkema, Rotterdam* (1994), 1-6.
- Ostermeier, R.M., "Deepwater Gulf of Mexico: A study of compaction effects on porosity and permeability," *Formation Evaluation*, (June 1993), 1-6.
- Spencer, J., "Frame moduli of unconsolidated sandstones," *Geophysics* (1994) **59**, No.9, 1263-1270.
- Cole, K.S., Cole, R.H., "Dispersion of dielectric constants," *Journal of Chemical Physics*, (1931) **1**, 270-274.
- Gross, B., "On creep and relaxation," *Journal of Applied Physics* (1947) **18**, 212-220.
- Thoegel, N.W., "The Phenomenological Theory of Viscoelastic Behavior: An Introduction," Berlin (1978), 39.
- Pusch, R., "Creep mechanisms in clay," *Creep and fracture*, ed: Easterling, K.

Appendix

The standard linear solid equations for creep and relaxation are given by

$$\epsilon = \left[\frac{1}{E_1} + \frac{1}{E_2} \left(1 - e^{-\frac{\tau}{t}} \right) \right] \sigma_0$$

and

$$\sigma = \epsilon_0 \cdot \left(\frac{E_1 E_2}{E_1 + E_2} + \frac{E_1^2}{E_1 + E_2} \cdot e^{-\left(\frac{E_1 + E_2}{E_2} \right) \frac{t}{\tau}} \right)$$

σ = 1-D stress

ϵ = 1-D strain

E_1 = outer spring (see Fig. 1)

E_2 = inner spring

σ_0 = stress perturbation

ϵ_0 = strain perturbation

t = time

τ = relaxation time constant

SI Metric Conversion Factors

in. x 2.54* E+00=cm

Tables

Table 1: The samples and their properties

Sample	Porosity	Mean grain size	Clay content (added by volume)	Grain morphology
Ottawa sand	34%	500 μm	5-10%	Rounded, well sorted
Wilm. sand	35-39%	300 μm	<10%	Angular, poorly sorted
Lentic sand	36%	100 μm	<5%	Angular, well sorted

Table 2: The creep parameters

Sample	Loading condition	Relaxation time (hours)	Pc (MPa)	σ _i (MPa)
Wilm.	uniaxial strain	13.0	30	40
Wilm.	triaxial stress	5.70	22	25
Lentic	uniaxial strain	0.37	15	18
Lentic	triaxial stress	1.88	10	18

Figures

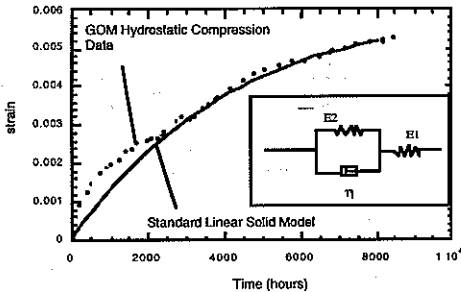


Fig 1.— A fit to hydrostatic creep data from an unconsolidated sand. This is a Gulf of Mexico sample fitted with a standard linear solid model. The fitting parameters give parameters necessary to predict the theoretical stress relaxation response³.

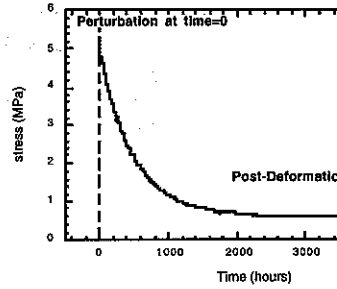


Fig 2.— Predicted theoretical stress relaxation experiment shown in Figure 1 assuming Following a step increase in strain, the trans away with time.

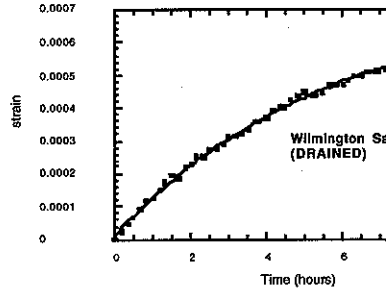


Fig 3.— Creep response of the Wilmington sand loading conditions. The solid line is an exponential fit. Pc=22MPa, σ_i=25MPa.

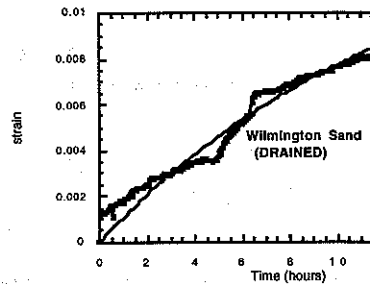


Fig 4.— Creep in the Wilmington sand loading conditions. The solid line is an exponential fit.

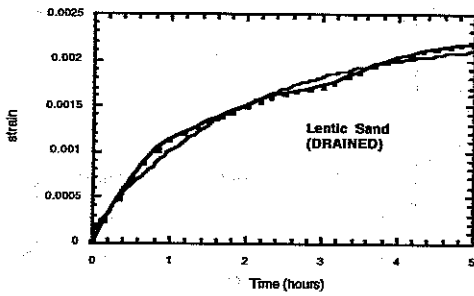


Fig 5.— Creep in the Lentic sand under triaxial loading conditions. The solid line is an exponential fit to the data.

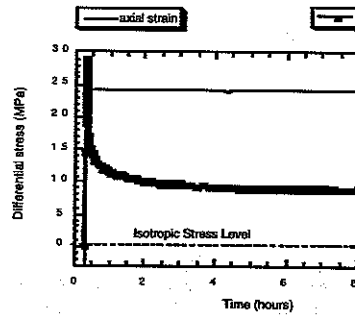


Fig 8.— Wilmington sand sample stress relaxation under triaxial loading conditions and constant axial strain.

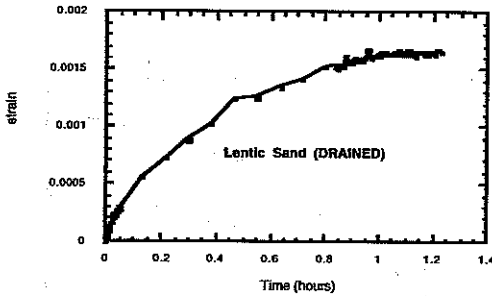
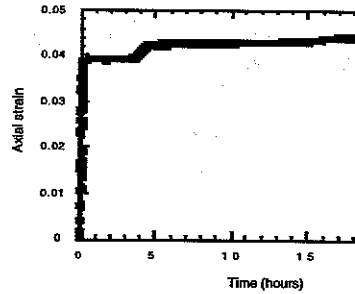


Figure 6.— Creep in the Lentic sand under uniaxial strain.



(a)

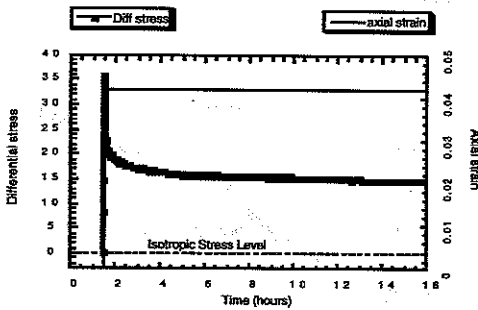
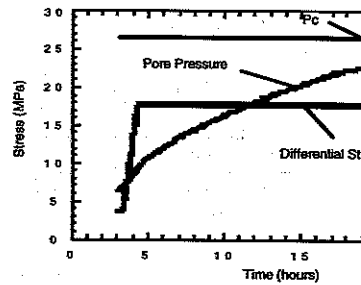
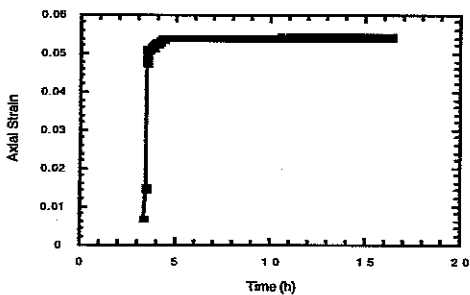


Fig 7.— Ottawa sand + 10% Montmorillonite clay stress relaxation under triaxial loading conditions and constant axial strain

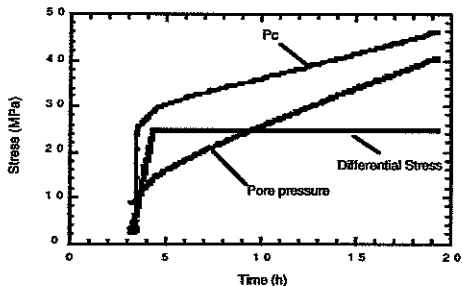


(b)

Fig— 9. (a) The strain history of the Lentic sand under compression. (b) The stress history of the same sand during a transient increase of pore pressure under constant axial strain.



(a)



(b)

Fig 10.— (a) The strain history of the uniaxial strain test on the Lentic sand subject to a step strain. (b) Following the step strain, both the pore pressure and confining pressure increase.

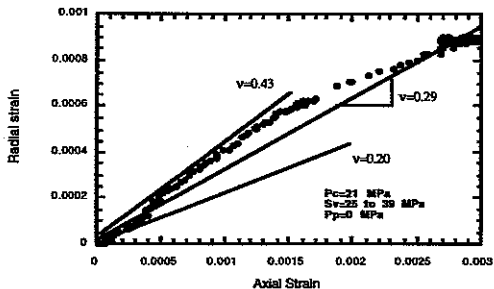


Fig 11.— The relationship between principle strains under triaxial compression of the Lentic sand.

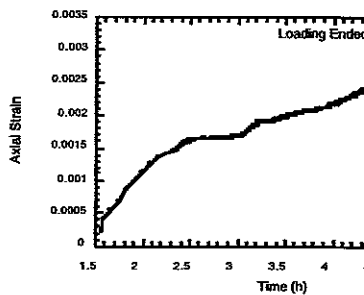


Fig 12.— Strain history of the uniaxial strain test on the Lentic sand. The stress ratio of the Lentic sand.

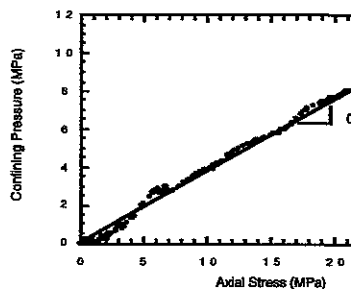


Fig 13.— The principle stresses of the Lentic sand under compression with a constant confining pressure.

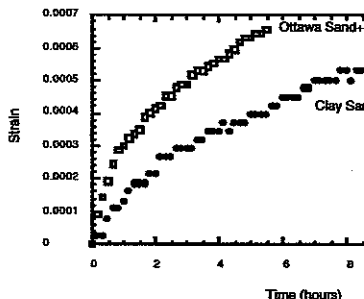


Fig 14.— The compression of pure clay discs and Ottawa sand (synthetic markers) compared to creep in a sample of Montmorillonite clay. Both samples are of the same clay.

The first part of the paper discusses the general theory of the subject, and the second part discusses the application of the theory to the case of the present study. The theory is based on the assumption that the system is in a state of equilibrium, and that the forces acting on the system are balanced. The application of the theory to the case of the present study shows that the system is in a state of equilibrium, and that the forces acting on the system are balanced.

The results of the present study show that the system is in a state of equilibrium, and that the forces acting on the system are balanced. This is in agreement with the theory, and with the results of previous studies. The present study also shows that the system is in a state of equilibrium, and that the forces acting on the system are balanced. This is in agreement with the theory, and with the results of previous studies.

The present study shows that the system is in a state of equilibrium, and that the forces acting on the system are balanced. This is in agreement with the theory, and with the results of previous studies. The present study also shows that the system is in a state of equilibrium, and that the forces acting on the system are balanced. This is in agreement with the theory, and with the results of previous studies.

The present study shows that the system is in a state of equilibrium, and that the forces acting on the system are balanced. This is in agreement with the theory, and with the results of previous studies. The present study also shows that the system is in a state of equilibrium, and that the forces acting on the system are balanced. This is in agreement with the theory, and with the results of previous studies.